LETTERS

Generation of single optical plasmons in metallic nanowires coupled to quantum dots

A. V. Akimov[1,4]*, A. Mukherjee[1]*, C. L. Yu[2]*, D. E. Chang[1], A. S. Zibrov[1,4], P. R. Hemmer[3], H. Park[1,2] & M. D. Lukin[1]

Control over the interaction between single photons and individual optical emitters is an outstanding problem in quantum science and engineering. It is of interest for ultimate control over light quanta[1], as well as for potential applications such as efficient photon collection[2], single-photon switching[3] and transistors[4], and long-range optical coupling of quantum bits[5,6]. Recently, substantial advances have been made towards these goals, based on modifying photon fields around an emitter using high-finesse optical cavities[2,3,5–8]. Here we demonstrate a cavity-free, broadband approach for engineering photon–emitter interactions[4,9] via subwavelength confinement of optical fields near metallic nanostructures[10–13]. When a single CdSe quantum dot is optically excited in close proximity to a silver nanowire, emission from the quantum dot couples directly to guided surface plasmons in the nanowire, causing the wire's ends to light up. Non-classical photon correlations between the emission from the quantum dot and the ends of the nanowire demonstrate that the latter stems from the generation of single, quantized plasmons. Results from a large number of devices show that efficient coupling is accompanied by more than 2.5-fold enhancement of the quantum dot spontaneous emission, in good agreement with theoretical predictions.

Surface plasmons, or surface plasmon polaritons, are propagating excitations of charge-density waves and their associated electromagnetic fields on the surface of a conductor[10]. Much like the optical modes of a conventional dielectric fibre, a broad continuum of surface plasmon modes can be confined on a cylindrical metallic wire and guided along the wire axis[12,13] (Fig. 1a). However, as opposed to dielectric waveguides[14,31], the thin wires can maintain propagation of

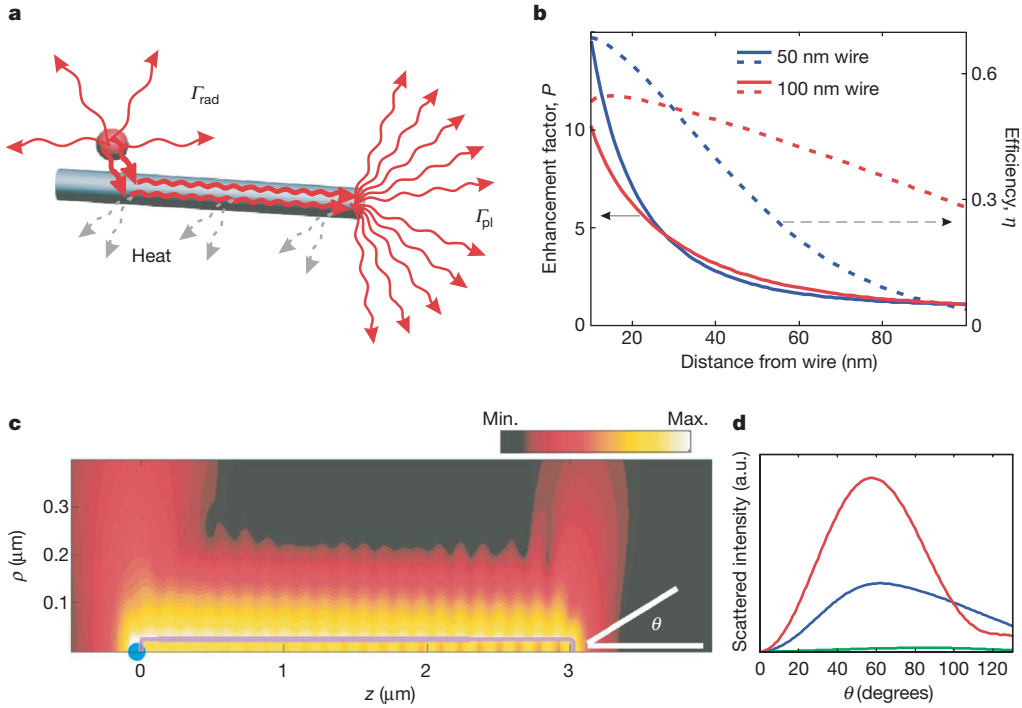

Figure 1 | Radiative coupling of quantum dots to conducting nanowires. a, A coupled quantum dot can either spontaneously emit into free space or into the guided surface plasmons of the nanowire with respective rates Γ_{rad}, Γ_{pl}. **b**, Theoretical dependence of the enhancement factor P (solid line) and efficiency of emission into surface plasmons (dashed line) on distance of the emitter from the nanowire edge. The red (blue) curve corresponds to a wire diameter of 100 nm (50 nm). **c**, Simulations of the electric field amplitude (arbitrary units) emitted by a dipole (blue filled circle) positioned 25 nm from one end of a conducting nanowire (whose surface is outlined) 3 μm in length and 50 nm in diameter. The vertical scale (ρ) is enlarged compared to the horizontal (z) to clearly show the near field of the surface plasmons. Upon hitting the far end of the nanowire, some of the surface plasmon energy is clearly scattered into the far-field, while the remaining is either lost to dissipation or to back-reflection. θ, Emission angle. **d**, Amplitude of the Poynting vector of the light scattered from the far end of the nanowire, as a function of θ (see **c**), for wires of diameter 100 nm (red curve), 50 nm (blue) and 25 nm (green).

[1]Department of Physics, [2]Department of Chemistry and Chemical Biology, Harvard University, Cambridge, Massachusetts 02138, USA. [3]Department of Electrical and Computer Engineering, Texas A&M University, College Station, Texas 77843, USA. [4]P.N. Lebedev Physical Institute RAS, Leninskiy prospect 53, Moscow, 119991, Russia.
*These authors contributed equally to this work.

surface plasmon modes localized transversely to dimensions comparable to the wire diameter d, even when it is much smaller than the optical wavelength λ. This subwavelength localization is accompanied by a dramatic concentration of optical fields[10,11]. In addition, the surface plasmon modes propagate with greatly reduced velocities because they involve the motion of charge-density waves[9,15,16].

The emission properties of a nanoscale optical emitter can be significantly modified by the proximity of a nanowire that supports surface plasmons. In principle, three distinct decay channels exist. First, direct optical emission into free-space modes is possible, with a rate modified from that of an isolated quantum dot owing to the proximity of the metallic surface[17]. Second, the optical emitter can be damped non-radiatively owing to ohmic losses in the conductor[17]. Last, and most importantly, the tight field confinement and reduced velocity of surface plasmons can cause the nanowire to capture the majority of spontaneous radiation into the guided surface plasmon modes[9], much like a lens with extraordinarily high numerical aperture. For an optical emitter placed within the evanescent surface plasmon mode tail, the spontaneous emission rate into the surface plasmons[9] is proportional to $(\lambda/d)^3$. In contrast, the free-space emission rate can be enhanced by at most a factor of four, whereas non-radiative damping becomes significant only for very small wire–emitter separation[9]. Thus, for an optimally placed emitter, the spontaneous emission rate Γ_{pl} into surface plasmons can far exceed the radiative and non-radiative rates (Γ_{rad} and Γ_{nrd}, respectively), which results in highly efficient coupling to surface plasmons and enhancement of the total decay rate (Γ_{total}) compared to that of an uncoupled emitter (Γ_0). This enhancement can be characterized by a Purcell factor, $P = \Gamma_{total}/\Gamma_0$, which for thin wires is predicted to be large[9]. We emphasize that this strong coupling is caused by the geometrical effect of tight confinement of the surface plasmons, and occurs far away from the plasmon resonance frequency of nanowires[18]. It does not involve an optical cavity[2,3,5–8], and can be achieved simultaneously over a broad continuum of optical frequencies.

Chemically synthesized CdSe quantum dots[19] placed proximally to silver nanowires comprise a simple experimental system to investigate the emitter–surface plasmon coupling. As illustrated in Fig. 1a, the spontaneous emission of a quantum dot is split between photon emission into free space, which can be detected by an optical microscope, and the excitation of surface plasmons (Γ_{nrd} is negligible for our chosen parameters, as described below). During propagation along the smooth nanowire, surface plasmons do not couple to the observable far-field modes of the surrounding dielectric. However, much like a conventional antenna, an abrupt end of the wire can scatter surface plasmons radiatively into far-field modes, thus facilitating their detection using an optical microscope. A simulation of this effect is shown in Fig. 1c, where a quantum dot is placed 25 nm away from one wire end: whereas the surface plasmons decay evanescently away from the nanowire edge, substantial emission into free space results from surface plasmon scattering at the far end of the wire. Silver nanowires were prepared using a solution-phase polyol method with modifications for surface passivation[20] (Supplementary Information). The samples were created by spinning quantum dots onto a glass substrate, covering them with an ~30-nm layer of poly (methylmethacrylate) (PMMA; see Supplementary Information for detailed analysis of the PMMA layer), and then depositing dry wires on top. Finally, the sample was overcoated with a thick layer of PMMA. Scanning electron microscopy images revealed that the diameters of the silver nanowires were 102 ± 24 nm (Supplementary Information). The closest allowed distance between the quantum dots and nanowires is determined by the thickness of the PMMA layer and the quantum dot shell radius (~5 nm), and is ~35 nm (Methods and Supplementary Information). The experimental set-up for studying the quantum dot–nanowire system (Fig. 2a) is based on a modified confocal microscope with three scanning channels. One channel (I) was used for imaging nanowires, and the second channel (II) was used for imaging quantum dots. The third channel (III), which can independently image any diffraction-limited spot within the field of view of the objective lens, was used to detect the scattered surface plasmons from the nanowire ends.

In general, the coupling between an optical emitter and single surface plasmons should be stronger for thinner wires[9] (Fig. 1b). However, for thinner wires, the out-coupling efficiency of surface plasmons to the far-field at the wire end decreases owing to a large wavevector mismatch. In this case, significant surface plasmon reflection at the nanowire ends causes standing surface plasmon wave

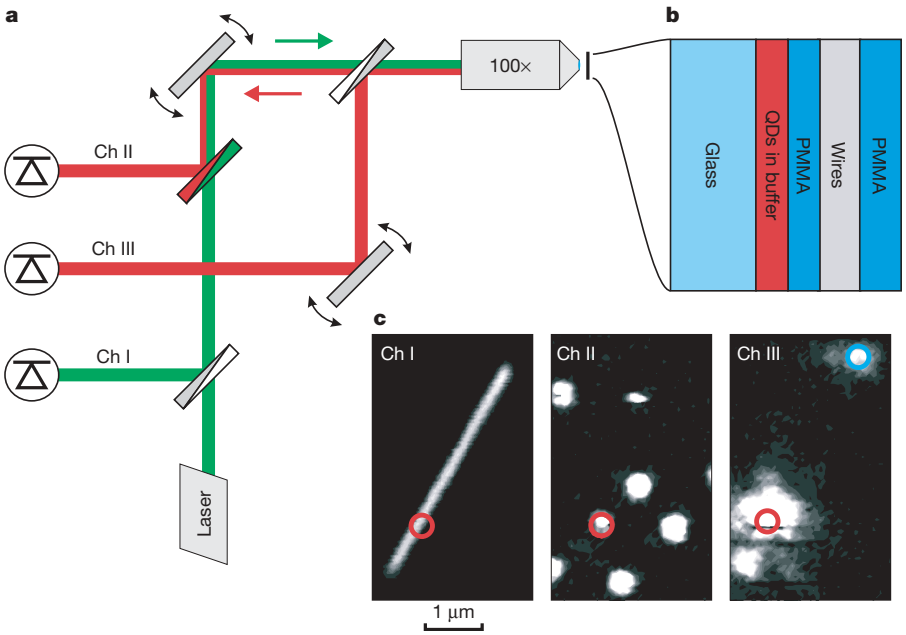

Figure 2 | Experimental set-up. a, Three-channel confocal microscope with 532 nm laser excitation source. **b**, Layout of sample containing quantum dots and nanowires. **c**, Left, channel I: nanowire image. Middle, channel II: image of quantum dots. The red circle denotes the position of the coupled quantum dot, and the same point is also denoted in the leftmost image. Right, channel III: the excitation laser was focused on the quantum dot (red circle). The largest bright spot corresponds to the quantum dot fluorescence, while two smaller spots correspond to surface plasmons scattered from the nanowire ends. The blue circle indicates the farthest end of the nanowire, used for photon cross-correlation measurements.

formation within the nanowire[12] (Fig. 1c) and eventual energy loss due to heating (ohmic losses). The effect of nanowire diameter on out-coupling efficiency is illustrated in Fig. 1d, where the intensity of the scattered radiation from the wire end is plotted for different wire diameters. For a 25-nm nanowire, hardly any scattering is seen from the end despite the stronger coupling between the emitter and surface plasmons, but the scattering is significant for a 100-nm wire (this was verified experimentally by exciting surface plasmons directly with a laser focused at one wire end; Supplementary Information). Nanowires with $d \approx 100$ nm exhibit both reasonable emitter–surface plasmon couplings and surface plasmon to far-field scattering, and thus were chosen for the experiments. The large bandwidth of the surface plasmon–emitter coupling enables us to perform the experiments at room temperature, where a single quantum dot spectral width exceeds 15 nm (Supplementary Information).

Figure 2c presents an experimental demonstration of directed emission of a quantum dot into surface plasmons. The leftmost panel shows a confocal reflection image of a silver nanowire recorded with channel I. The middle panel corresponds to a fluorescence image of quantum dots detected at 655 nm with channel II. These two images were used to determine the positions of the nanowire and quantum dot relative to each other. Owing to the resolution limit of our optical system, the actual distance between a quantum dot and the nanowire could not be determined, and only quantum dots that appear directly on top of a nanowire were chosen for experiment. The rightmost panel shows a coupled wire–dot system imaged with channel III. When the proximal quantum dot (circled in red) was excited by the laser, the nanowire ends literally lit up. The large spot around the red circle corresponds to emission from the quantum dot itself, whereas the two other points coincide with the wire ends. Significantly, a high degree of correlation was seen between the time traces of the fluorescence counts from the quantum dot and the end of the coupled wire (Fig. 3a). These observations indicate that the source of the fluorescence from the wire end is the quantum dot.

Photon coincidence measurements[1] of the quantum dots (Fig. 3b) demonstrate that these quantum dots can only emit a single photon at a time. In these measurements, the free-space fluorescence from the quantum dot was equally split into two channels using a beam splitter and detected by avalanche photo-diodes. The coincidences between two channels were recorded as a function of time delay τ. If the quantum dot emits only one photon at a time it can only be recorded at one of the channels, and therefore zero coincidences are expected between the two channels at $\tau = 0$, as seen in Fig. 3b. The slight offset from zero can be attributed to stray light, dark counts of the detectors and the resolution limit of the electronics (Supplementary Information).

The light emission at the nanowire end is a result of single, quantized surface plasmons scattering off the ends of the nanowire. This is demonstrated in Fig. 3c by the dip at $\tau = 0$ in the photon coincidence measurements between the free-space fluorescence of the quantum dot and emission from the wire end. This near-zero coincidence is a consequence of the fact that the single photon emitted from a quantum dot can either radiate into free space or the surface plasmon modes, but never both simultaneously.

Data presented in Fig. 3, along with measured count rates, can be used to quantify the coupling strength of the quantum dot to the surface plasmons. As this coupling creates a new decay channel for the quantum dot, its decay rate is expected to increase. To study this enhancement, observed coincidence data were fitted to a simple two-level model of quantum dot emission[21] (Fig. 3b; see also Supplementary Information). The model incorporates an incoherent pumping rate R from the ground to an excited state of a quantum dot and a decay rate Γ_{total} back to the ground state. In this model, the temporal width of the anti-bunching dip is given by $\Delta\tau = \ln\sqrt{2}/(R+\Gamma_{\text{total}})$, where the excitation rate R is proportional to the incident power. Therefore, by extracting $\Delta\tau$ from coincidence measurements as a function of incident laser power and extrapolating to $R = 0$, Γ_{total} can be obtained (Fig. 4a).

The natural lifetimes of individual dots (20–30 ns) vary owing to the heterogeneity in their structures. However, a comparison of the lifetime distributions of 30 coupled and 100 uncoupled quantum dots (Fig. 4b) clearly demonstrates that statistically the lifetime (decay rate) of the exciton in coupled quantum dots is shortened (enhanced). The average lifetime of the coupled (uncoupled) quantum dots was found to be 13 ± 4 ns (22 ± 5 ns). At the same time, the distribution for coupled quantum dots has a larger weight towards shorter lifetimes. Specifically, certain coupled and uncoupled quantum dots exhibited lifetimes as short as 6 ns and 15 ns, respectively, indicating that $P > 2.5$ is achieved for some coupled quantum dot–nanowire systems. The apparent efficiency of emission into the surface plasmons can be estimated by comparing the ratio of photon counts (n) obtained directly from the dot and from the wire ends, $\eta_{\text{m}} \approx n_{\text{ends}}/(n_{\text{dot}} + n_{\text{ends}})$, and is found to be ~27% for the best coupled quantum dot–nanowire system (Fig. 4c and Supplementary Information). This value does not account for the surface plasmons that are dissipated before they reach the wire ends. Correcting for the measured average absorption lengths in our nanowires allows us to deduce that the actual efficiency approaches $\eta \approx 60 \pm 10\%$ (Supplementary Information), directly demonstrating

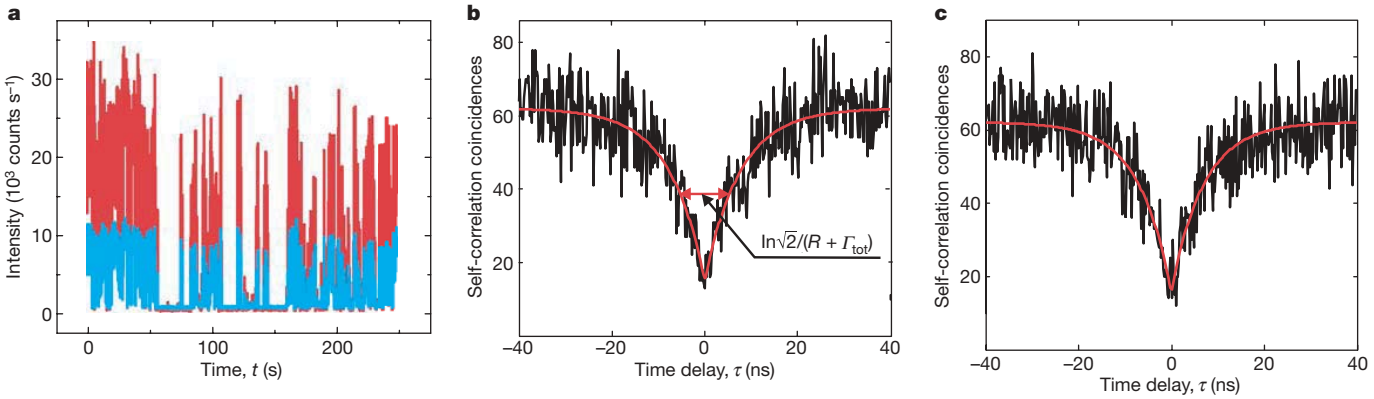

Figure 3 | Demonstration of single surface plasmon generation. **a**, Time trace of fluorescence counts (red curve) from a coupled quantum dot and scattered light (blue) from the end of the coupled nanowire. Fluctuations are due to quantum dot blinking[19]. **b**, Second-order correlation function $G^{(2)}(\tau)$ of quantum dot fluorescence. The number of coincidences at $\tau = 0$ goes almost to zero, confirming that the quantum dot is a single-photon source. The width of the dip depends on Γ_{total} and the pumping rate R as shown. **c**, Second-order cross-correlation function between fluorescence of the quantum dot and scattering from the nanowire end, obtained by coincidences between channel II (quantum dot) and channel III (wire end). The black and red traces in **b**, **c** indicate experimental data and best fits, respectively.

very efficient coupling to surface plasmons. We note that this coupling efficiency significantly exceeds that recently observed between atoms and dielectric nanofibres[14,31].

The broadband nature of the strong coupling is demonstrated by comparing the optical spectra associated with emission from the quantum dot and from the wire end. For individual dots randomly drawn from an inhomogeneous ensemble with $\lambda = 655 \pm 15$ nm, we find that both the quantum dot and wire-end emission exhibit identical ~15-nm-wide spectra. This is consistent with the ability of metallic wires to guide a broad range of optical frequencies[22] and with theoretical predictions (Supplementary Information) that strong coupling can be obtained for a broad continuum of frequencies away from the peak of the observed plasmon resonances[18].

Further insight into the quantum dot–surface plasmon coupling can be obtained by comparing our experimental observations with detailed electrodynamic calculations[9]. Our model of quantum dot emission near a silver nanowire embedded in a dielectric medium includes losses as well as multiple surface plasmon modes. Figure 1b shows the total spontaneous emission rates and the efficiency $\eta = \Gamma_{pl}/\Gamma_{total}$ for single surface plasmon generation as a function of quantum dot distance from the wire ($d = 50$ and 100 nm). Here the polarization of the quantum dot transition was selected to be radially oriented, because this direction is expected to yield the dominant contribution to enhancement. For quantum dots positioned 35 nm from the wire and for a 100 nm wire, the calculation yields a Purcell factor $P \approx 3.7$. The lower enhancement observed experimentally can be attributed to the contributions from other polarizations and the random positioning of the quantum dots away from the wire. For this distance of separation, the non-radiative decay rate ($\Gamma_{nrd} < 0.05\Gamma_0$) is predicted to be negligible (Supplementary Fig. 10). In addition to enhanced emission into surface plasmon modes, our theory also predicts a moderate increase in the radiative emission rate, a well-known phenomenon for dipoles oriented perpendicularly to a metallic surface[17]. For 100 nm wires and 35 nm nanowire–quantum dot distances, the surface plasmon generation efficiency η is theoretically estimated to be ~50%, which is consistent with our observations.

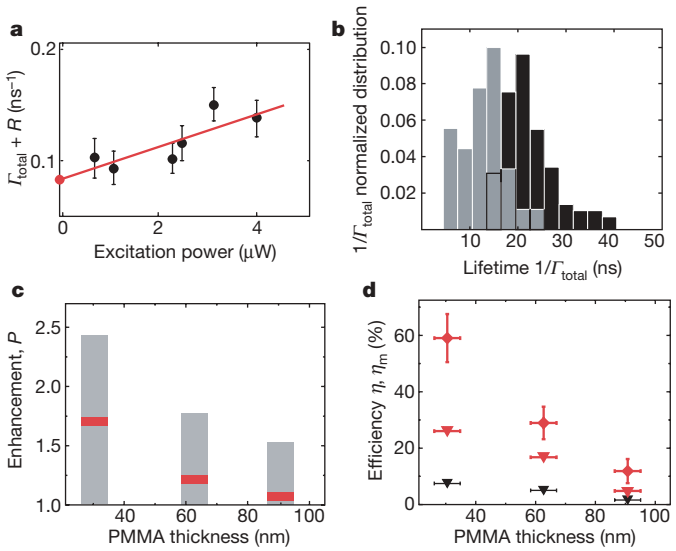

Figure 4 | Characterization of quantum dot–nanowire coupling. a, The linear dependence of $G^{(2)}$ width on laser power (black filled circles) is extrapolated to zero power (red filled circle), yielding Γ_{total} of a quantum dot. The laser power is proportional to the incoherent pumping rate R of the dot. **b**, Normalized histograms of quantum dot lifetimes. The black (grey) bars denote the distribution of uncoupled (coupled) quantum dots. Overlapping parts of the histograms are indicated by outlined and vertically stacked bars. **c**, Average Purcell enhancement, P, versus PMMA thickness. Red line, average value of P. Height and width of grey bars indicate the standard deviations of P and PMMA thickness, respectively. **d**, Measured maximum and average efficiencies of emission into the surface plasmons versus PMMA thickness. Black (red) filled triangles, average (maximum) apparent coupling efficiencies η_m, without compensating for surface plasmon losses. Red filled diamonds, maximum actual efficiency η, after compensating for dissipation. Error bars in **a**, **c**, **d** indicate ± 1 s.d.

Further comparison with theoretical predictions is obtained by repeating our observations with thicker PMMA layers (Fig. 4c, d). These measurements demonstrate that both enhancement and estimated coupling efficiency rapidly decrease as the minimum quantum dot–nanowire spacing increases, and become very small for PMMA thicknesses above 100 nm. These observations are also in good agreement with the above theoretical predictions. The large variances in the Purcell factors obtained for different devices are due primarily to variations in the distance between quantum dots and nanowires beyond the minimum allowed distance set by the PMMA layer thickness.

The unique properties of nanoscale surface plasmons have recently been explored in a variety of fascinating systems, from transmission through subwavelength structures[11] to biomedical devices[10] and proposals for realizing 'perfect' lenses and invisibility cloaks[10]. Enhancement of fluorescence[23,24], polarization-dependent coupling[25,26] and normal mode splitting[27,28] near subwavelength structures have also recently been observed. The present work extends these developments in two principal directions. First, we have shown experimentally and theoretically that the present approach results simultaneously in significant enhancement of surface plasmon emission and efficient collection into guided modes propagating along a well-defined direction. Second, it establishes direct coupling between individual emitters and individual, quantized surface plasmons. It thus bridges the fields of nanoscale plasmonics and quantum optics, and opens up the possibility of using quantum optical techniques to achieve new levels of control over the interaction of single surface plasmons and to realize novel quantum plasmonic devices.

In the current set-up, the benefits of using smaller wires must be balanced against poor out-coupling to free-space modes. However, this trade-off can be circumvented by using optimized geometries and evanescent out-coupling to mode-matched optical fibres[9,16,23]. The excellent coupling expected from these integrated systems can be used, for example, for efficient single-photon sources, high resolution microscopy[29,30] and sensing[20], or long-range quantum bit coupling[5]. Furthermore, in such systems an individual emitter can be made optically opaque to single incident surface plasmons, which can be used to produce large optical nonlinearities for realization of single-photon transistors[4]. Beyond these specific applications, the ability to create and control individual quanta of current oscillating at optical frequencies and accompanied by guided radiation with subwavelength localization opens up intriguing new possibilities at the interface of optics and electronics.

METHODS SUMMARY

Samples were prepared by spin-coating a solution of chemically synthesized CdSe quantum dots (mixed with $Na_2B_4O_7$ and cysteine) onto a plasma-cleaned glass slide at 3,000 r.p.m. for 60 s under a nitrogen atmosphere. Three minutes later, PMMA (1, 2 and 3 wt% in toluene for 30, 60 and 90 nm films) was spun on top at 6,000 r.p.m. for 60 s. The quantum dots used do not dissolve in toluene and are unperturbed during the spin-coating process (experimentally, we find that the arrangement of quantum dots on the surface remains unchanged). A stamp with the modified silver nanowires was placed on top of the slide and pressed for a few seconds. The stamp was left there for 20 min and then gently peeled off, leaving nanowires on the PMMA. Finally, PMMA (2.2 wt%) was spun on top at 1,000 r.p.m. for 60 s (Fig. 2b).

Our confocal microscope uses a c.w. 532 nm laser as the excitation source. It is focused onto the sample using a Nikon CFI Plan Fluor 100× oil immersion objective NA 1.3, while a mirror mounted on a galvanometer is used to scan the incoming beam. Channel II acts as a confocal microscope and is used to image single quantum dots, via fluorescence at 655 nm. Channel I is combined with channel II using a 90:10 beam splitter that directs part of the reflected laser light towards a detector and can be used to image the silver nanowires. Channel III is combined with the main set-up using a 50:50 beam splitter and is an independent

imaging system. It also includes a galvanometer which allows us to image any diffraction limited spot within the field of view to detect fluorescence at 655 nm. Additional details of our experimental set-up are provided in Supplementary Information.

Received 10 April; accepted 4 September 2007.

1. Haroche, S. & Raimond, J.-M. *Exploring the Quantum: Atoms, Cavities, Photons*. (Oxford Univ. Press, New York, 2006).
2. Englund, D. *et al.* Controlling the spontaneous emission rate of single quantum in a two-dimensional photonic crystal. *Phys. Rev. Lett.* **95,** 013904 (2005).
3. Birnbaum, K. M. *et al.* Photon blockade in an optical cavity with one trapped atom. *Nature* **436,** 87–90 (2005).
4. Chang, D. E., Sørensen, A. S., Demler, E. A. & Lukin, M. D. A single-photon transistor using nano-scale surface plasmons. *Nature Phys.* advance online publication doi:10.1038/nphys708 (26 August 2007).
5. Cirac, J. I., Zoller, P., Kimble, H. J. & Mabuchi, H. Quantum state transfer and entanglement distribution among distant nodes in a quantum network. *Phys. Rev. Lett.* **78,** 3221–3224 (1997).
6. Imamoğlu, A. *et al.* Quantum information processing using quantum dot spins and cavity QED. *Phys. Rev. Lett.* **83,** 4204–4207 (1999).
7. Hennessy, K. *et al.* Quantum nature of a strongly coupled single quantum dot–cavity system. *Nature* **445,** 896–899 (2007).
8. Wilk, T., Webster, S. C., Kuhn, A. & Rempe, G. Single-atom single-photon quantum interface. *Science* **317,** 488–490 (2007).
9. Chang, D. E., Sørensen, A. S., Hemmer, P. R. & Lukin, M. D. Quantum optics with surface plasmons. *Phys. Rev. Lett.* **97,** 053002 (2006).
10. Atwater, H. A. The promise of plasmonics. *Sci. Am.* **296,** 56–63 (2007).
11. Genet, C. & Ebbesen, T. W. Light in tiny holes. *Nature* **445,** 39–46 (2007).
12. Sanders, A. W. *et al.* Observation of plasmon propagation, redirection, and fan-out in silver nanowires. *Nano Lett.* **6,** 1822–1826 (2006).
13. Ditlbacher, H. *et al.* Silver nanowires as surface plasmon resonators. *Phys. Rev. Lett.* **95,** 257403 (2005).
14. Nayak, K. P. *et al.* Optical nanofiber as an efficient tool for manipulating and probing atomic fluorescence. *Opt. Express* **15,** 5431–5438 (2007).
15. Takahara, J., Yamagishi, S., Taki, H., Morimoto, A. & Kobayashi, T. Guiding of a one-dimensional optical beam with nanometer diameter. *Opt. Lett.* **22,** 475–477 (1997).
16. Chang, D. E., Sørensen, A. S., Hemmer, P. R. & Lukin, M. D. Strong coupling of single emitters to surface plasmons. *Phys. Rev. B* **76,** 035420 (2007).
17. Chance, R. R., Prock, A. & Silbey, R. Molecular fluorescence and energy transfer near interfaces. *Adv. Chem. Phys.* **37,** 1–65 (1978).
18. Sun, Y., Gates, B., Mayers, B. & Xia, Y. Crystalline silver nanowires by soft solution processing. *Nano Lett.* **2,** 165–168 (2002).
19. Chung, I., Witkoskie, J. B., Cao, J. & Bawendi, M. G. Description of the fluorescence intensity time trace of collections of CdSe nanocrystal quantum dots based on single quantum dot fluorescence blinking statistics. *Phys. Rev. E* **73,** 011106 (2006).
20. Tao, A. *et al.* Langmuir-Blodgett silver nanowire monolayers for molecular sensing using surface-enhanced Raman spectroscopy. *Nano Lett.* **3,** 1229–1233 (2003).
21. Lounis, B., Bechtel, H. A., Gerion, D., Alivisatos, P. & Moerner, W. E. Photon antibunching in single CdSe/ZnS quantum dot fluorescence. *Chem. Phys. Lett.* **329,** 399–404 (2000).
22. Dickson, R. M. & Lyon, L. A. Unidirectional plasmon propagation in metallic nanowires. *J. Phys. Chem. B* **104,** 6095–6098 (2000).
23. Hochberg, M., Baehr-Jones, T., Walker, C. & Scherer, A. Integrated plasmon and dielectric waveguides. *Opt. Express* **12,** 5481–5486 (2004).
24. Biteen, J. S., Lewis, N. S. & Atwater, H. A. Spectral tuning of plasmon-enhanced silicon quantum dot luminescence. *Appl. Phys. Lett.* **88,** 131109 (2006).
25. Zhang, J., Ye, Y.-H., Wang, X., Rochon, P. & Xiao, M. Coupling between semiconductor quantum dots and two-dimensional surface plasmons. *Phys. Rev. B* **72,** 201306(R) (2005).
26. Mertens, H., Biteen, J. S., Atwater, H. A. & Polman, A. Polarization-selective plasmon-enhanced silicon quantum-dot luminescence. *Nano Lett.* **6,** 2622–2625 (2006).
27. Bellessa, J., Bonnand, C. & Plenet, J. C. Strong coupling between surface plasmons and excitons in an organic semiconductor. *Phys. Rev. Lett.* **93,** 036404 (2004).
28. Dintinger, J., Klein, S., Bustos, F., Barnes, W. L. & Ebbesen, T. W. Strong coupling between surface plasmon-polaritons and organic molecules in subwavelength hole arrays. *Phys. Rev. B* **71,** 035424 (2005).
29. Klimov, V. V., Ducloy, M. & Letokhov, V. S. A model of an apertureless scanning microscope with a prolate nanospheroid as a tip and an excited molecule as an object. *Chem. Phys. Lett.* **358,** 192–198 (2002).
30. Smolyaninov, I. I., Elliott, J., Zayats, A. & Davis, C. C. Far-field optical microscopy with a nanometer-scale resolution based on the in-plane magnification by surface plasmon polaritons. *Phys. Rev. Lett.* **94,** 057401 (2005).
31. Sagué, G., Vetsch, E., Alt, W., Meschede, D. & Rauschenbeutel, A. Cold atom physics using ultra-thin optical fibers: light-induced dipole forces and surface interactions. Preprint at ⟨http://arxiv.org/quant-ph/0701167⟩ (2007).

Supplementary Information is linked to the online version of the paper at www.nature.com/nature.

Acknowledgements We acknowledge discussions with M. Loncar, J. Doyle, A. Sørensen and M.-H. Yoon, and support from the NSF, DARPA, Harvard-MIT CUA, Harvard CNS, the DTO, the Packard Foundation and Samsung Electronics.

Author Information Reprints and permissions information is available at www.nature.com/reprints. Correspondence and requests for materials should be addressed to M.D.L. (lukin@fas.harvard.edu) and H.P. (Hongkun_Park@harvard.edu).